Polymer(Korea), Vol. 41, No. 3, pp. 452-459 (2017)
https://doi.org/10.7317/pk.2017.41.3.452

ISSN 0379-153X(Print)
ISSN 2234-8077(Online)

제조 방법에 따른 70PC/30ABS/GO 복합체의 GO 분산성 및 기계적 물성

신경민 · 박주영 · 김연철†

공주대학교 신소재공학부 고분자공학전공

(2016년 10월 18일 접수, 2016년 11월 24일 수정, 2016년 11월 26일 채택)

GO Dispersion and Mechanical Properties of 70PC/30ABS/GO Composites according to Fabrication Methods

Ghoung Min Shin, Ju Young Park, and Youn Cheol Kim†

Major in Polymer Science and Engineering, Kongju National University, Cheonan 31080, Korea

(Received October 18, 2016; Revised November 24, 2016; Accepted November 26, 2016)

초록: 제조방법에 따른 폴리카보네이트(polycarbonate, PC)/아크릴로니트릴-부타디엔-스티렌 공중합체(acrylonitrile-butadiene-styrene copolymer, ABS)/그래핀 옥사이드(graphene oxide, GO) 복합체(composite)의 GO 분산성과 물성을 고찰하기 위해 이축압출기(twin screw extruder)를 이용하여 PC/ABS/GO 복합체를 제조하였다. 열역학적인 GO의 위치는 접촉각 측정과 젖음 계수를 이용하여 ABS 상내와 ABS-*g*-MA에 존재하려는 경향을 확인하였으며, 제조방법에 상관없이 대부분의 GO가 ABS 상내에서 관측됨을 TEM 결과로 확인하였다. 인장강도(tensile strength)와 아이조드 충격강도(Izod impact strength)를 비교한 결과 PC/GO 복합체를 이용한 PC-GO/ABS 복합체의 물성 개선효과가 우수하게 나타났다. PC/GO 복합체를 이용하여 스크류 속도를 변화시켜 제조한 PC-GO/ABS 복합체의 경우 스크류 속도가 증가함에 따라 인장강도와 충격강도가 소폭 증가함을 확인하였다. SEM과 TEM 결과로부터 스크류 속도가 증가할수록 압출기 내 체류시간이 작아 GO가 PC와 ABS 계면에 많이 분포되어 있는 것을 확인하였다.

Abstract: PC/ABS/GO composites were fabricated using a twin screw extruder in order to study GO dispersion and the physical properties of polycarbonate (PC)/acrylonitrile-butadiene-styrene copolymer (ABS)/graphene oxide (GO) composites depending on fabrication methods. The position of the GO was thermodynamically identified by measurement of contact angle and the use of wetting coefficient. The GO tended to be located in the ABS phase and ABS-*g*-MA. In TEM images, most of the GO was located in the ABS phase regardless of fabrication methods. In comparisons of tensile strength and Izod impact strength, the physical properties of PC-GO/ABS composites using PC/GO composites were significantly improved. In PC-GO/ABS composites produced by using PC/GO composites, and changing screw rpm, tensile strength and impact strength slightly increased as screw rpm rose. In SEM and TEM images, it was confirmed that GOs were mostly dispersed in the PC and ABS interface due to the short residence time in the extruder as screw rpm rose.

Keywords: graphene oxide, immiscible PC/ABS blend, dispersion, fabrication method.

Introduction

Polymer composites are polymer materials that have been physically or chemically mixed with fillers, such as metal powder, natural fiber, carbon fiber, carbon nanotubes (CNT) and graphene, in order to achieve high performance and overcome the limitations of the physical properties of the polymers. Fillers can greatly improve the mechanical strength, gas barrier properties, wear resistance and heat resistance of polymer composites, compared to the original polymers. Many studies on highly functional polymer composites are being conducted by combining carbon-based fillers, such as CNT, carbon fiber and graphene, with polymer.[1-3] Among them, graphene is receiving particular attention.

Graphene, which is composed of sp2-bonded carbon atoms, has a unique and honeycomb shaped structure with thickness as thin as a single atom. The process of graphene exfoliation from graphite was introduced by Geim and Novoselov *et al*. in the UK in 2004.[4] Graphene has a high specific surface area, high Young's modulus, as well as great heat conductivity, elec-

†To whom correspondence should be addressed.
E-mail: younkim@kongju.ac.kr

trical conductivity and mechanical properties.[5-8] Graphene provides great physical properties when used as a filler for polymers, and is being studied widely for application in various areas including the fields of electronics, aeronautical engineering and automotive engineering.[9,10] However, graphene also has a strong van der Waals force, which enables it to form stable chemical structures with strong cohesive force, but as a consequence, its dispersion in polymers is difficult, and its mechanical properties are highly reduced because it also causes voids and cracks in polymer composites.[11] On the other hand, graphene oxide (GO), is graphene with attached oxygen functional groups such as epoxy groups, hydroxyl groups or carboxyl groups, and as a result of those groups the cohesive force of GO is weaker than that of graphene, and dispersion can be enhanced in a polymer matrix containing polar groups.[12-14] When a carbon filler is mixed with an immiscible polymer blend, its electrical properties and mechanical properties depend on the distribution of the filler, and the most effective method to enhance these properties is to distribute the carbon filler uniformly in the polymer matrices. A number of recent studies on methods for adding carbon filler to immiscible polymer blends have been conducted.[15-19] Among immiscible polymer blends, a blend of PC/ABS has been widely investigated. The PC/ABS blend is an immiscible polymer which has the advantages of both ABS (chemical resistance, fluidity and low price) and PC (mechanical strength and heat resistance).[15] The PC/ABS blend has received attention after commercialization because products can be produced with a range of physical properties just by adjusting the PC/ABS ratio, without the need to add other polymers.

Y. Sun *et al*.[16] studied the electric resistance of such composites depending on the rubber content in ABS and the position of MWCNTs (multi-walled carbon nanotubes) in a PC/ABS blend. J. Chen *et al*.[17] predicted the position of CNTs by using a wetting coefficient to locate CNTs in the PC/ABS interface using PC, ABS and ABS-g-MA, which is a compatibilizer. In addition, C. Mao *et al*.[19] reported an effective method for optimizing the aggregation and distribution of graphene in immiscible PS/PMMA blends by selectively locating the graphene in any one phase.

As mentioned above, the location of the graphene is a very important factor in immiscible polymer blend systems such as PC/ABS blends. However, studies on changes in physical properties depending on the position of GO in PC/ABS/GO composites are rare.

Thus, we produced the 70PC/30ABS/GO composite using several GO insertion methods(direct insertion, PC-GO, ABS-GO) and several different extruder screw rpm. We then identified the position of GO by using a wetting coefficient, and used SEM and TEM observations to investigate changes in physical properties depending on the position of the GO. ABS-*g*-MA, which is a compatibilizer, showed the optimum impact strength at a concentration of 5 phr (parts per hundred resins) in our previous study on 70PC/30ABS,[20] and therefore the content of compatibilizer was set at 5 phr.

Experimental

Materials and Methods. GO used in the study was purchased from IDT International (GO 4401, Korea) and prepared according to Hummer's methods. The PC was from Samyang Corporation (TRIREX® 3025, Korea) and its melt index (MI) was 9 g/10 min. ABS was obtained from Cheil Industries Inc. (BC-0140H, Korea) and its MI was 10.5 g/10 min. Maleic anhydride (99%, Junsei) was used to prepare a compatibilizer and dicumyl peroxide (98%, Sigma-Aldrich) was used as an initiator.

Preparation of PC/ABS/GO Composites. The ABS-*g*-MA compatibilizer was prepared by using a twin screw extruder (L/D = 36, BauTeck, Korea) with ABS, 5 wt% MAH (maleic anhydride) and 0.3 wt% DCP (dicumyl peroxide) as an initiator at 230 ºC (die)/250 ºC (barrel)/180 ºC (hopper) and at 20 rpm through reactive extrusion. Before preparation of the composite, PC and ABS were fully dried in a vacuum oven at 70 ºC. There were two steps for preparing the composite. In the first step, PC-GO and ABS-GO composites were prepared. Extrusion temperature was 250 ºC (die)/260 ºC (barrel)/200 ºC (hopper) for the PC-GO composites and 230 ºC (die)/240 ºC (barrel)/180 ºC (hopper) for ABS-GO composites. Screw rpm was set at 50. The content of GO in the composite was 1.43 wt% in PC-GO and 2.31 wt% in ABS-GO. In the second step, prepared PC-GO and ABS-GO with PC, ABS and ABS-*g*-MA were used to make a PC/ABS ratio of 70/30, GO content of 1 wt% and ABS-*g*-MA 5 phr. Then, the PC-GO/ABS and PC-GO/ABS/ABS-*g*-MA composites were prepared at 230 ºC (die)/240 ºC (barrel)/180 ºC (hopper) and at 50 rpm. In addition, the screw rpm was changed to 50, 100, 150 and 200 rpm during preparation of the composites in order to analyze the position of GO depending on residence time in the extruder.

Measurements. A universal testing machine (UTM, Hounsfield, H10KS, UK) was used to determine the sample

tensile strength. The cross-head speed was set to 10 mm/min and the mechanical test curves were obtained from the dumbbell shape specimens type ASTM D 638. The impact strength was measured by using an Izod impact tester (Daeyeong C&T, Korea) after preparing and notching 2 mm specimens (ASTM D 256). A 1 mm plate of PC and ABS was prepared by using a hot-press in order to predict the position of GO in the PC/ABS composite based on the wetting coefficient. GO was made as a film and the contact angle was measured by contact angle measurement (Phoenix, SEO, Korea) to determine surface tension. Distilled water (H_2O),which is a polar solvent, and diiodomethane (CH_2I_2), which is a non-polar solvent, were used for determining the surface tension. A field-emission scanning electron microscope (FE-SEM, Mira3, TESCAN, the Czech Republic) and a field-emission transmission electron microscope (FE-TEM, JEM-2100F, JEOL, Japan) were used to identify the dispersion of GO and its position in the composites. SEM microscope was used to observe a section of the sample coated with gold sputter. A microtome was used to make 70 nm film specimens, and acceleration voltage in the TEM was 200 kV. Dynamic rheological measurement (MCR 301, Aton Paar, Austria) was used to measure viscoelastic behaviors of the composites at 240 °C and 100-0.01 1/s (frequency), using a parallel plate which was 25 mm in diameter. The strain was set as 4% and the gap size was 0.9 mm. Based on the result of the strain sweep test, the strain was fixed as 4% where the linear form was maintained. The specimens were prepared by using a hot-press at 240 °C. The surface resistances were measured at room temperature at a voltage source level of 800 V and discharging time of 30 sec using a digital ultra-high resistance/micro current meter (8340A). The sample dimension was 80×80×2 mm. The MI was measured by using a melt flow tester manufactured by Coad 1001 of Ocean science in Korea following ASTM D 1238. Each composite was pressed with 1.2 kg load at 300 °C and the weight passed through an orifice for 10 min was measured.

Results and Discussion

In general, the interface of two phases in immiscible polymers, or the position of a filler in one specific phase, can be predicted by using thermodynamic factors. According to Young's equation, the position of a filler in the equilibrium state can be calculated by using a wetting coefficient (ω_a).[16]

$$\omega_a = \frac{\gamma_{\text{filler-B}} - \gamma_{\text{filler-A}}}{\gamma_{\text{A-B}}} \quad (1)$$

$\gamma_{\text{filler-A}}$ is the interfacial tension between a filler and polymer A, and $\gamma_{\text{filler-B}}$ is the interfacial tension between a filler and polymer B. $\gamma_{\text{A-B}}$ is the interfacial tension between polymer A and polymer B. If a wetting coefficient is higher than 1, a filler is located in the polymer A phase. If it is between -1 and 1, a filler is located in the interface of two polymer phases. If it is lower than -1, a filler is located in the polymer B phase.

The interfacial tension can be calculated by the harmonic-mean eq. (2).[17]

$$\gamma_{12} = \gamma_1 + \gamma_2 - 4\left(\frac{\gamma_1^d \gamma_2^d}{\gamma_1^d + \gamma_2^d} + \frac{\gamma_1^p \gamma_2^p}{\gamma_1^p + \gamma_2^p}\right) \quad (2)$$

γ_i is the surface energy of component i. γ_i^d is a non-polar part (dispersive, d) of the surface energy of component i and γ_i^p is a polar part (polar, p). Surface energy was determined using the Owens-Wendt-geometric equation with a program after measuring a contact angle.

The measured contact angles and surface energy (γ) for each component are shown in Table 1. The interfacial tension between the components and the wetting coefficient are presented in Table 2. The interfacial tension was calculated by using eq. (2) and the wetting coefficient was computed by using eq. (1) with the interfacial tension obtained with eq. (2). As a result, the interfacial tension of PC-ABS, PC-GO, ABS-GO, ABS-ABS-*g*-MA and ABS-*g*-MA-GO were found to be 0.04, 15.47, 14.87, 1.24 and 10.75 mN/m, respectively. The

Table 1. Contact Angle and Surface Energy Data of Component

Sample	Contact angle (°)		γ (mN/m)	γ^d (mN/m)	γ^p (mN/m)
	H_2O	CH_2I_2			
PC	30.13	21.33	47.03	46.73	0.3
ABS	89.62	23.68	46.28	45.86	0.41
ABS-*g*-MA	81.22	23.99	47.01	44.83	2.06
GO	64.72	49.53	44.12	30.97	12.97

Table 2. Interfacial Tension and Wetting Coefficient of Component

Component	Interfacial tension (mN/m)	Wetting coefficient
PC-ABS	0.04	-14.26 (PC/ABS)
PC-GO	15.47	
ABS-GO	14.87	
ABS-ABS-*g*-MA	1.24	-3.31 (ABS/ABS-*g*-MA)
ABS-*g*-MA-GO	10.75	

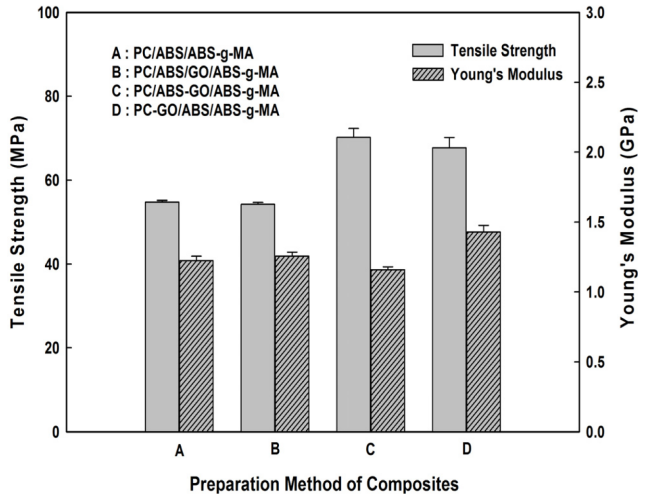

Figure 1. Tensile strengths and Young's moduli of PC/ABS/GO/ABS-*g*-MA composites.

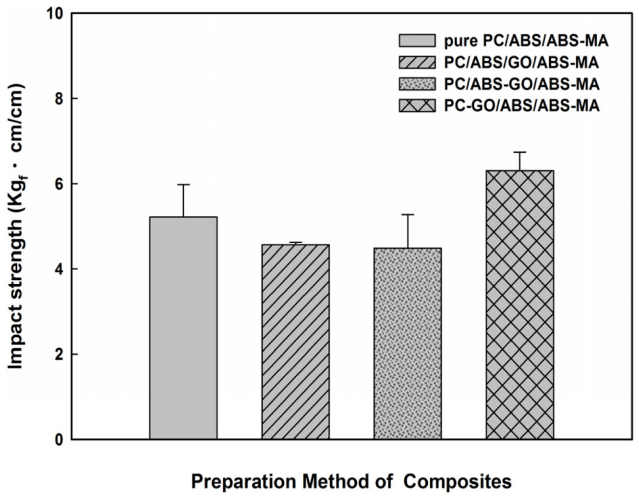

Figure 2. Impact strengths of PC/ABS/GO/ABS-*g*-MA composites.

wetting coefficient of PC-ABS was -14.26 and it was thermodynamically predicted that GO might be located in the ABS phase. The wetting coefficient of ABS-ABS-*g*-MA was -3.31, suggesting that GO might be located in ABS-*g*-MA.

Thermodynamically, the GO in PC/ABS/GO composites might be located in the ABS phase and ABS-*g*-MA. Thus, it was suggested that insertion methods, residence time in the extruder and the presence of a compatibilizer might have an effect on the GO dispersion and physical properties of PC/ABS/GO composites. We conducted a study on this.

We used UTM to identify the tensile properties of the composites prepared by different GO insertion methods. The tensile strength and Young's modulus depending on GO insertion methods are shown in Figure 1. When ABS-*g*-MA was used as a compatibilizer and GO was directly inserted into PC/ABS/GO/ABS-*g*-MA, the tensile properties were not different from those in the case of PC/ABS. However, they were improved in PC/ABS-GO/ABS-*g*-MA and PC-GO/ABS/ABS-*g*-MA. This may be because the dispersion of GO was better in the PC/ABS-GO/ABS-*g*-MA and PC-GO/ABS/ABS-*g*-MA composites, where GO was preliminarily mixed as a master batch, than in PC/ABS/GO/ABS-*g*-MA where GO was directly inserted, and therefore tensile strength was high.

The Izod impact strength of the composites depending on insertion methods is shown in Figure 2. In the composite with directly inserted GO and the composite using ABS-GO, impact properties were lower than those in PC/ABS/ABS-*g*-MA whereas the impact strength of the PC-GO/ABS/ABS-*g*-MA composite was 6.31 kgf·cm/cm, which is a 20% improvement compared to that of PC/ABS/ABS-*g*-MA. This improvement may be because GO moved to the ABS phase, a thermodynamically stable phase, in the extruder, during insertion of PC-GO, and therefore dispersion was improved. The dispersion properties of GO were additionally confirmed by

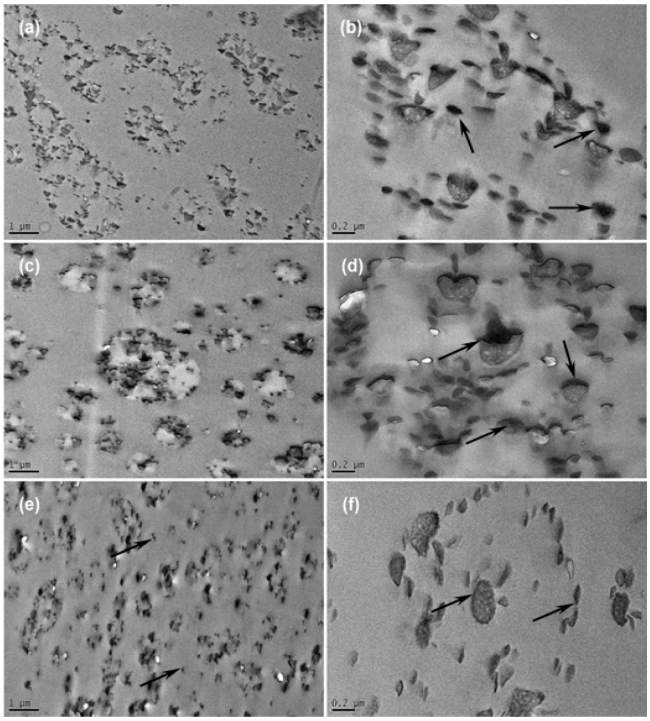

Figure 3. TEM images of the composites with different processing parameters: (a) and (b) are for PC/ABS/GO/ABS-*g*-MA; (c) and (d) are for PC/ABS-GO/ABS-*g*-MA; (e) and (f) are for PC-GO/ABS/ABS-*g*-MA.

Table 3. Melt Flow Index and Surface Resistance of PC/ABS/GO/ABS-*g*-MA Composites

Component	Melt index (g/10 min)	Surface resistivity (Ω/sq)
PC/ABS/ABS-*g*-MA	1.54	9.61E+15
PC/ABS/GO/ABS-*g*-MA	1.73	1.82E+15
PC/ABS-GO/ABS-*g*-MA	1.52	1.80E+15
PC-GO/ABS/ABS-*g*-MA	2.48	7.25E+14

TEM observations as shown in Figure 3. In this figure, the round phase is the ABS phase and the rest of the area is the PC phase. GO is identified by arrows. The TEM image of the PC-GO/ABS/ABS-*g*-MA composite, compared to other composites, shows that the GO was well distributed in both phases. Based on this result, it was suggested that the dispersion properties of GO would be the best with the insertion of PC-GO. In that case, the mechanical properties would be great. The MI and surface resistances of the composites were summarized in Table 3. In case of PC-GO/ABS/ABS-*g*-MA composite, molecular weight and surface resistance showed lower value than the other composites. This is the other evidence that GO dispersion would be the best in case of insertion of PC-GO.

The rheological properties of polymer/nanofiller composites are extremely affected by microstructure, such as the dispersion of the nanofiller. Therefore, rheological properties are an effective means for predicting the dispersion of a nanofiller in polymers.[21-23] The *G′*-*G″* plot depending on GO insertion methods is shown in Figure 4(a) and complex viscosity is presented in Figure 4(b). Compared to the other composites, the PC-GO/ABS/ABS-*g*-MA composite showed a *G′*-*G″* pattern close to PC, suggesting that the GO was well distributed. The shape of the complex viscosity was also close to PC, compared to that of other composites, also suggesting that GO was well distributed.

In the investigation of mechanical and rheological properties of the composites based on GO insertion methods, the strongest effects were produced by the GO insertion methods that affected the dispersion of GO during preparation of the PC/ABS/GO composites, and that affected the physical properties of the PC-GO/ABS composite. Accordingly, changes in the dispersion properties and mechanical properties of GO depending on the application of a compatibilizer, and residence time, were studied for the PC-GO/ABS composite.

The Izod impact strength depending on application of a compatibilizer and screw rpm is shown in Figure 5. As shown

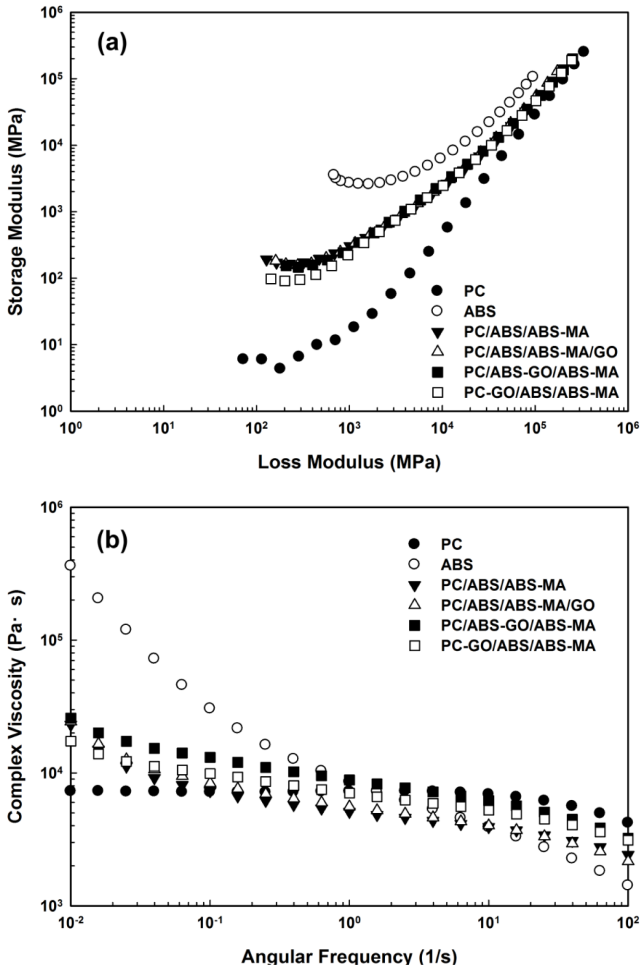

Figure 4. Rheological properties of PC/ABS/GO/ABS-*g*-MA composites: (a) *G′*-G″ plot; (b) complex viscosity.

in Figure 5(a), the impact strength of the immiscible PC-GO/ABS composite without added compatibilizer was 4.00-5.15 kgf·cm/cm, which is much higher than the 1.48 kgf·cm/cm of PC/ABS, depending on screw rpm. This is because GO acts as a compatibilizer in the PC/ABS interface. In previous studies, it was reported that GO could perform the role of compatibilizer in the PA/poly(phenylene oxide) (PPO) interface because PPO was adsorbed into the carbon structure of the GO, and the affinity of the oxygen functional groups of GO with polyamide.[24]

As residence time was increased (that is, screw rpm was decreased), the GO inserted in the PC phase was thermodynamically expected to move to the interface and then the ABS phase. When GO was located in the interface, miscibility should be the greatest. At 200 rpm, a relatively low residence time, GO was located in the interface and therefore the impact

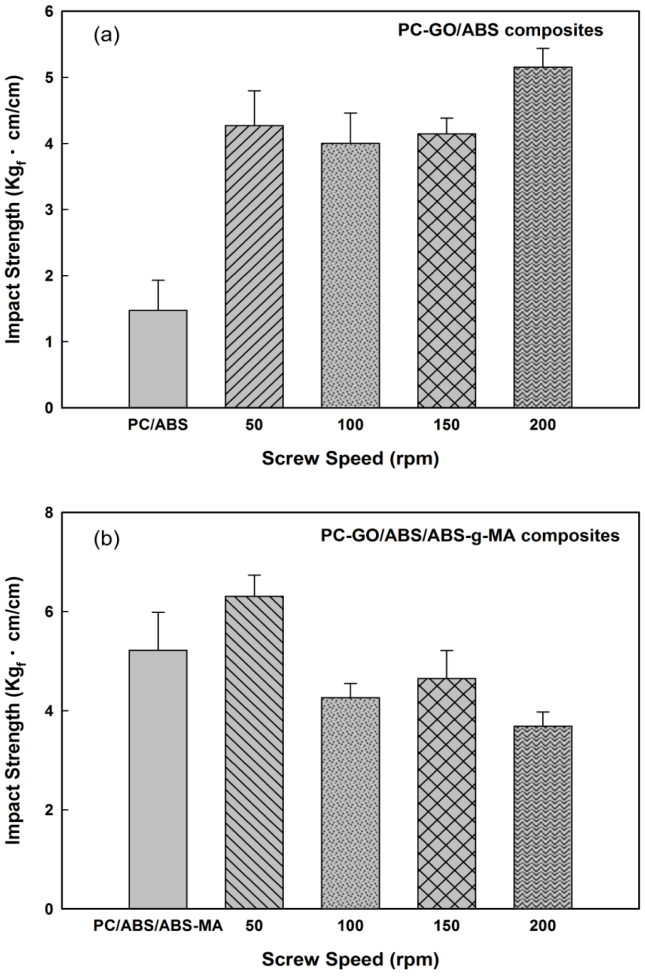

Figure 5. Impact strengths of the composites as a function of screw rpm: (a) PC-GO/ABS; (b) PC-GO/ABS/ABS-*g*-MA.

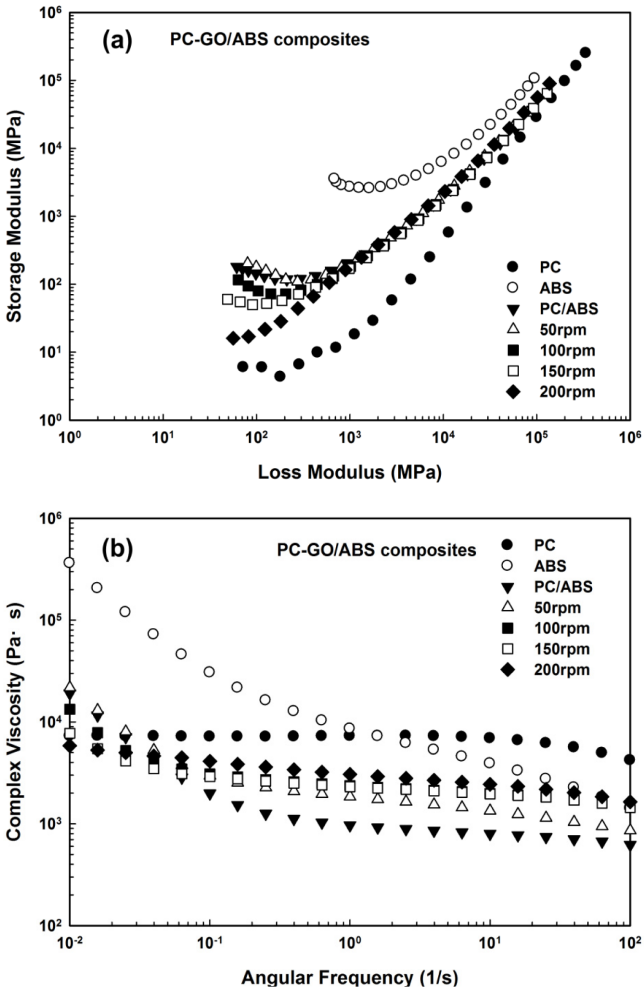

Figure 6. Rheological properties of PC-GO/ABS composites: (a) *G′*-*G″* plot; (b) complex viscosity.

strength should be the highest. As shown in Figure 5(b), unlike immiscible PC-GO/ABS composites, the impact strength of PC-GO/ABS/ABS-*g*-MA, in which a compatibilizer had been applied, was improved as screw rpm was decreased. This might be because the GO in the interface hinders miscibility at high rpm and relatively low residence time. In addition, the impact properties at 50 rpm might be improved because the GO had completely moved and dispersed to the ABS phase, thus enhancing the impact properties of the ABS.

The *G′*-*G″* plot of immiscible PC-GO/ABS composites depending on screw rpm is shown in Figure 6(a). At 200 rpm, the behavior in the low frequency area was similar to that of pure PC. In contrast, as screw rpm was decreased, the pattern was comparable to that of pure ABS. As mentioned above, GO which was located in the PC/ABS interface due to short residence time at high screw rpm, moved to the ABS phase as screw rpm was reduced. In Figure 6(b), complex viscosity behaviors also show a similar result.

The *G′*-*G″* plot of the PC-GO/ABS/ABS-g-MA composite depending on screw rpm is shown in Figure 7(a). In contrast to the immiscible composites, the pattern was not different and an opposite trend was even observed. At high screw rpm, GO was located around the compatibilizer, reducing miscibility. At low screw rpm, GO moved to the ABS phase, and ABS-*g*-MA performed the role of compatibilizer. The complex viscosity in Figure 7(b) shows a similar pattern.

SEM images of the PC-GO/ABS composite depending on screw rpm are shown in Figure 8. Images of PC-GO/ABS composites prepared at 50, 100, 150 and 200 rpm are shown in Figure 8(a), (b), (c) and (d), respectively. In the images, the phase is round and has many voids. It is the ABS phase which is the dispersion phase. The rough section is the PC phase

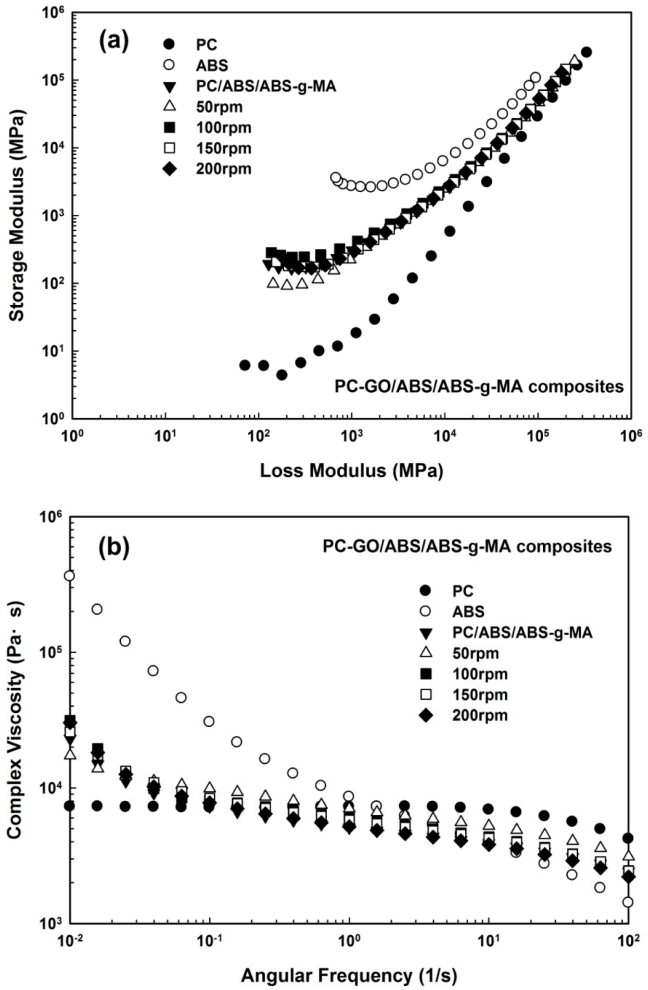

Figure 7. Rheological properties of PC-GO/ABS/ABS-*g*-MA composites: (a) *G′*-*G″* plot; (b) complex viscosity.

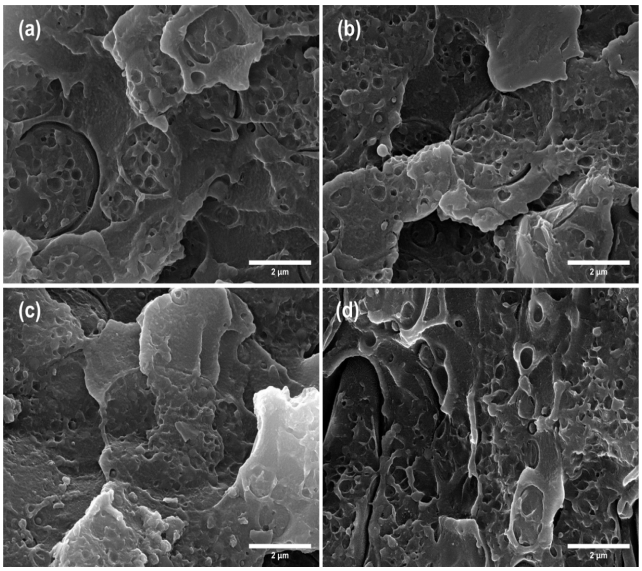

Figure 8. SEM images of PC-GO/ABS composites with different screw speed: (a) 50 rpm; (b) 100 rpm; (c) 150 rpm; (d) 200 rpm.

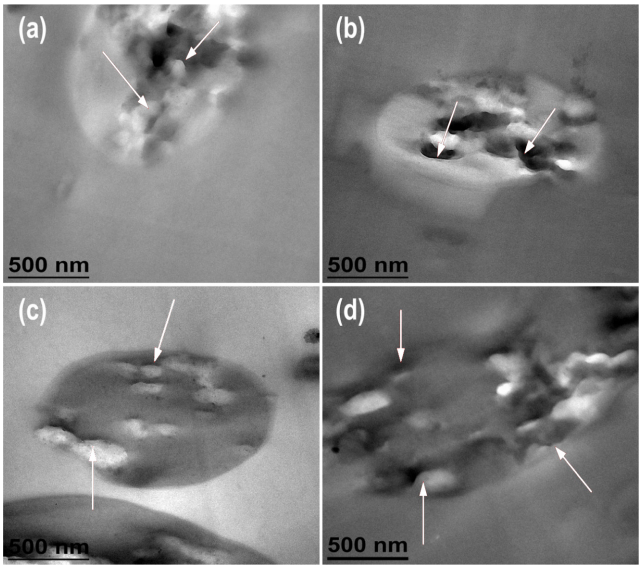

Figure 9. TEM images of PC-GO/ABS composites with different screw speed: (a) 50 rpm; (b) 100 rpm; (c) 150 rpm; (d) 200 rpm.

which is the continuous phase. The size or shape of the ABS phase did not change when screw rpm was increased. However, the interface between the ABS phase and the PC phase became ambiguous at higher screw rpm. In Figure 8(d), the 200 rpm composite, it is hard to distinguish the phase. This might be because GO was close to the PC/ABS interface at higher screw rpm and therefore miscibility increased.

The position of the GO in the PC-GO/ABS composite was identified by TEM for more precise observation, and the result is shown in Figure 9. Images of PC-GO/ABS composites prepared at 50, 100, 150 and 200 rpm are shown in Figure 9(a), (b), (c) and (d), respectively. The round phase is the ABS phase, which is the dispersion phase. The rest of the area is the PC phase which is the continuous phase. GO is indicated by the arrows.

In the TEM images, GO is located in the ABS phase, as predicted by wetting coefficient. As the screw rpm increased, GO moved closer to the ABS/PC interface. This is because processing at high screw rpm was completed before the GO was stabilized in the ABS phase. Sufficient time is required thermodynamically for stabilization of the GO moving to the ABS phase.[21] Therefore, it was confirmed that GO near the PC/ABS interface had a miscible effect, and therefore the impact strength increased.

Conclusions

In this study, a wetting coefficient was used to confirm that GO was thermodynamically located in the ABS phase, and in ABS-*g*-MA. The correlation between mechanical properties, and the position of GO in the PC/ABS/GO composite, was investigated for different GO insertion methods, screw rpm and application of a compatibilizer. In the evaluation of tensile properties and impact properties, the PC-GO/ABS/ABS-*g*-MA composite using PC-GO was the best, which might be related to the dispersion and the position of GO in the composite. The impact strength of the PC-GO/ABS composite was improved as screw rpm rose. This might be because of the miscible effect of GO, which was confirmed by rheological properties and electron microscope. In contrast, the impact strength of the PC-GO/ABS/ABS-*g*-MA composite, in which ABS-*g*-MA was applied as a compatibilizer, was reduced as screw rpm increased. The miscible effect decreased as screw rpm rose, as confirmed by the *G′*-*G″* plot and complex viscosity. SEM and TEM were used to identify the position of GO in the PC-GO/ABS composite depending on screw rpm. As screw rpm was increased, the PC/ABS interface became ambiguous in the SEM images, and GO became closer to the PC/ABS interface in the TEM images. Furthermore, in the PC-GO/ABS/ABS-*g*-MA composite, the GO was located in the ABS-*g*-MA, and therefore the miscible effect was rather reduced.

Acknowledgments: This research was supported by Basic Science Research Program through the National Research Foundation of Korea (NRF) funded by the Ministry of Education, Science and Technology (No.: 2012R1A1A2003989) and the Human Resources Development program (No. 20154030200940) of the Korea Institute of Energy Technology Evaluation and Planning (KETEP) grant funded by the Korea government Ministry of Trade, Industry and Energy.

References

1. O. K. Park, S. Lee, B. C. Ku, and J. H. Lee, *Polym. Sci. Techn.*, **22**, 467 (2011).
2. Z. Y. Xiong, L. Wang, Y. Sun, Z. X. Guo, and J. Yu, *Polymer*, **54**, 447 (2013).
3. G. Mittal, V. Dhand, K. Y. Rhee, S. J. Park, and W. R. Lee, *J. Ind. Eng. Chem.*, **21**, 11 (2015).
4. A. K. Geim and K. S. Novoselov, *Nature Mat.*, **6**, 183 (2007).
5. Y. T. Liu, X. M. Xie, and X. Y. Ye, *Carbon*, **49**, 3529 (2011).
6. Y. Zhu, S. Murali, W. Cai, X. Li, J.W. Suk, J. R. Potts, and R. S. Ruoff, *Adv. Mater.*, **22**, 3906 (2010).
7. J. Du and H. M. Cheng, *Macromol. Chem. Phys.*, **213**, 1060 (2012).
8. G. K. Ramesha and S. Sampath, *J. Phys. Chem. C*, **113**, 7985 (2009).
9. R. Surudžić, A. Janković, M. Mitrić, I. Matić, Z. D. Juranić, L. Živković, V. Mišković-Stanković, K. Y. Rhee, S. J. Park, D. Hui, M. Mitrić, I. Matić, Z. D. Juranić, and L. Živković, *J. Ind. Chem. Eng.*, **34**, 250 (2016).
10. S. Stankovich, D. A. Kikin, G. H. B. Dommett, K. M. Kohlhaas, E. J. Jimney, E. A. Stach, R. D. Piner, S. T. Nguyen, and R. S. Ruoff, *Nature*, **442**, 282 (2006).
11. J. Zhu, J. Lim, C. H. Lee, H. I. Joh, H. C. Kim, B. Park, N. H. You, and S. Lee, *J. Appl. Polym. Sci.*, **131**, 40177 (2014).
12. A. Yasmin, J. Luo, and I. M. Daniel, *Compo. Sci. Techno.*, **66**, 1182 (2006).
13. S. T. Kim and H. J. Choi, *Appl. Chem.*, **41**, 2106 (2005).
14. P. Ding, S. Su, N. Song, S. Tang, Y. Liu, and L. Shi, *Carbon*, **66**, 576 (2014).
15. K. H. Song, J. H. Hong, Y. T. Sung, Y. H. Kim, M. S. Han, H. G. Yoon, and W. N. Kim, *Polym. Korea*, **31**, 283 (2010).
16. Y. Sun, Z. X. Guo, and J. Yu, *Macromol. Mater. Eng.*, **295**, 263 (2010).
17. J. Chen, Y. Y. Shi, J. H. Yang, N. Zhang, T. Huang, C. Chen, Y. Wang, and Z. W. Zhou, *J. Mater. Chem.*, **22**, 22398 (2012).
18. R. H. Pour, A. Hassan, M. Soheilmoghaddam, and H. C. Bidsorkhi, *Polym. Compo.*, **37**, 1633 (2014).
19. C. Mao, Y. Zhu, and W. Jiang, *ACS Appl. Mater. Interfaces*, **4**, 5281 (2012).
20. J. Y. Park, B. Y. Lee, H. J. Cha, and Y. C. Kim, *Appl. Chem. Eng.*, **26**, 173 (2015).
21. J. Huang, C. Mao, Y. Zhu, W. Jiang, and X. Yang, *Carbon*, **73**, 267 (2014).
22. W. Marcin, A. Benedito, and E. Gimenez, *J. Appl. Polym. Sci.*, **131**, 40271 (2014).
23. D. Ren, S. Zheng, F. Wu, W. Yang, Z. Liu, and M. Yang, *J. Appl. Polym. Sci.*, **131**, 39953 (2014).
24. Y. Cao, J. Zhang, J. Feng, and P. Wu, *ACS Nano*, **5**, 5920 (2011).